 Transactions on Modelling and Simulation vol 10, © 1995 WIT Press, www.witpress.com, ISSN 1743-355X

Marangoni effects on drop deformation in an extensional flow: the role of surfactant physical chemistry

Y. Pawar, K.J. Stebe
Department of Chemical Engineering, The John Hopkins University, 3400 N. Charles Street, Baltimore, MD 21218, USA

Abstract

The interface of a droplet in an extensional flow moves both tangentially and normally. When surfactants are adsorbed on the drop interface, Marangoni stresses, which resist tangential shear, and Marangoni elasticities, which resist surface dilatation, develop. In this paper, the dependence of these effects on surfactant physical chemistry, and their impact on drop deformation are probed. Repulsive or cohesive interactions between surfactant molecules change the surface equation of state which dictates the sensitivity of the surface tension to adsorbed surfactant. For example, cohesion decreases this sensitivity, favoring strong surface concentration gradients. Boundary Element results are presented for fluids of equal viscosities containing an insoluble surfactant.

1 Introduction

An initially spherical drop of radius a, suspended in an immiscible, neutrally buoyant, Newtonian fluid of equal viscosity μ, is subject to an extensional flow of strain rate G, causing it to elongate. (Taylor [1]) The surface tension of the interface is given by γ_o. In the absence of surfactant adsorption, the capillary number Ca alone governs the drop deformation.

$$Ca = \frac{\mu G a}{\gamma_o}$$

This group is the ratio of characteristic viscous stresses to surface tension. For weak flows, (small Ca), the drop deforms only slightly from a spherical geometry. (Barthes-Biesel & Acrivos [2]) As Ca increases, the steady shapes

are more elongated. For Ca in excess of a critical value Ca^{cr}, the drop elongates, ultimately fragmenting into smaller drops. (Rallison & Acrivos [3])

When a non-ionic surfactant is in the outer phase at concentration C_{eq}, it adsorbs on the quiescent drop interface, establishing a surface concentration Γ_{eq} and reducing the surface tension to γ_{eq}. When the extensional flow is initiated, a stagnation ring develops at the drop equator, and stagnation points appear at either pole.(see Fig. 1) Surface convection sweeps adsorbed surfactant toward the poles, causing a non-uniform surface concentration Γ which alters the flow via the stress balance at the interface: (Levich [4])

$$[\,[\boldsymbol{n}\cdot\underline{\boldsymbol{T}}]\,] = -\frac{\partial\gamma}{\partial\Gamma}\nabla_s\Gamma + 2H\gamma(\Gamma)\,\boldsymbol{n} \qquad (1)$$

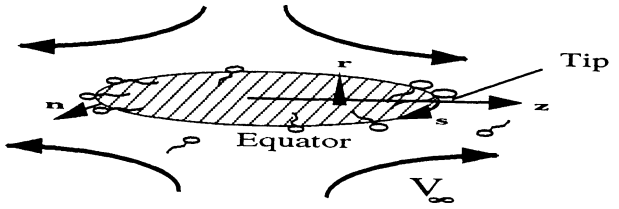

Figure 1 Flow Geometry

where $\underline{\mathbf{T}}$ is the Cauchy stress tensor, $\mathbf{n}$ is the surface normal, and the bracketed term on the left hand side of eqn (1) represents the stress jump at the interface. The local surface tension is denoted γ, ∇_s is the surface gradient operator, and 2H is the mean curvature of the interface. The interface pulls from the low surface tension zone at the poles toward the elevated tension at the equator, exerting a Marangoni stress, which is the first term on the right hand side of eqn (1). The normal stress balance is also altered, since regions of low surface tension require higher curvatures to balance the stress jump across the interface. This effect, the Marangoni elasticity, is the last term in eqn (1).

The surface tension dependence on the surface concentration is determined by the adsorption isotherm and its corresponding surface equation of state. Non-ideal interactions between surfactants (e.g. cohesion/repulsion) strongly impact the form of these expressions. (Lin et al. [5])

Numerical results on the impact of these interactions on deformation are presented in this paper. Below, the surfactant physical chemistry and dynamics, along with previous insoluble surfactant work in this flow are reviewed. Thereafter, our results for insoluble surfactants are presented.

2 Surfactants and Surface Stresses

For an insoluble surfactant, Γ is determined by the balance of surface convection and surface dilatation, which disturb the distribution, to the surface

diffusion flux, which tends to restore equilibrium: (Aris [6])

$$\frac{\partial \Gamma}{\partial t} + \nabla_s \cdot (\Gamma \boldsymbol{v_s}) - D_s \nabla_s^2 \Gamma = 0 \qquad (2)$$

where t denotes time, D_s is the surface diffusivity, and $\mathbf{v}_s$ is the surface velocity. This velocity has a normal component which dilutes Γ and a tangential component which creates surface gradients in Γ. The insoluble limit corresponds to dilute bulk concentrations where the scale for diffusive flux (DC_{eq}^2/Γ_{eq} , where D is the bulk diffusivity) is slow compared to the surface convective/dilatational flux ($G\Gamma_{eq}$).

Scaling Γ with Γ_{eq} and t with G^{-1}, eqn (2) in dimensionless form is:

$$\frac{\partial \Gamma'}{\partial t'} + \nabla_s \cdot (\Gamma' \boldsymbol{v_s'}) - \frac{1}{Pe_s} \nabla_s^2 \Gamma' = 0 \qquad (3)$$

where the primes indicate a dimensionless variable.

Scaling the Cauchy stress by μG, the curvature 2H by the inverse drop radius a^{-1}, γ by its clean interface value γ_o, and $\partial\gamma/\partial\Gamma$ by $RT\Gamma_\infty/\Gamma_{eq}$, (where Γ_∞ is the maximum packing of surfactant, R is the ideal gas constant and T is the temperature), eqn (1) becomes:

$$Ca\,[\,[\boldsymbol{n}\cdot\underline{\boldsymbol{T}}']\,] = -E\frac{\partial \gamma'}{\partial \Gamma'} \nabla_s \Gamma' + 2H'\gamma'(\Gamma')\,\boldsymbol{n} \qquad (4)$$

In these expressions, two additional dimensionless groups appear:

$$Pe_s = \frac{a^2 G}{D_s}\,;\; E = \frac{RT\Gamma_\infty}{\gamma_o}$$

- The surface Peclet number, Pe_s, is the ratio of characteristic convective to surface diffusive fluxes; this group determines the magnitude of the surface concentration gradients.
- The elasticity number E is a measure of the sensitivity of the surface tension to the surface concentration; this group couples the local surface concentration to the local surface tension.

The adsorptive/desorptive flux of surfactant from an interface is given by:

$$-\boldsymbol{n}\cdot\boldsymbol{j}_{ads} = \beta C_s \exp^{\frac{-\epsilon_a}{RT}} (\Gamma_\infty - \Gamma) - \alpha \exp^{\frac{-\epsilon_d}{RT}} \Gamma \qquad (5)$$

where β, (α) is the characteristic kinetic constant for adsorption, (desorption), and C_s is the concentration in the sublayer immediately adjacent to the interface. The energies ϵ_a and ϵ_d are activation energies for adsorption and desorption, respectively. At equilibrium, the adsorptive flux is zero, establishing the adsorption isotherm. For long chain saturated surfactants (e.g. the n-alcohols, [cf 5]), ϵ_a and ϵ_d depend upon Γ because of cohesive interactions among the saturated chains. For bulky sidechains, repulsive interactions have been observed. Keeping only linear terms, the energies are:

$$\epsilon_i = \epsilon_{io} + \nu_i \Gamma \qquad (6)$$

where i =a,d respectively. The adsorption isotherm and corresponding surface equation of state are the Frumkin equations:

$$\frac{\Gamma_{eq}}{\Gamma_\infty} = \frac{k_f}{e^{\left(\frac{K\Gamma_{eq}}{\Gamma_\infty}\right)} + k_f} \qquad (7)$$

$$\frac{\gamma}{\gamma_o} = 1 + E\left(\ln\left[1 - \frac{\Gamma}{\Gamma_\infty}\right] - \frac{K}{2}(\Gamma/\Gamma_\infty)^2\right) \qquad (8)$$

where the adsorption constant k_f and the interaction parameter K are:

$$k_f = \frac{\beta C_{eq}}{\alpha} e^{\frac{-(\epsilon_{ao} - \epsilon_{do})}{RT}} ; \qquad K = \frac{(\nu_a - \nu_d)\Gamma_\infty}{RT}$$

K is negative for cohesion, positive for repulsion. These non-ideal interactions strongly alter the partitioning of surfactant between the bulk and interface, (see Fig. (2a)) (Lin et al. [5]). For a given C_{eq}, the $\Gamma_{eq}/\Gamma_\infty$ are greater for cohesion, smaller for repulsion relative to the Langmuir case.

The surface equation of state, eqn (8) is assumed to relate $\gamma(\Gamma(s))$ even when the interface is not at equilibrium. This relationship therefore dictates the impact of the surfactant on the flow field. It is graphed in Fig. 2(b) as a function of scaled area/molecule $\Gamma_{eq}^{-1}\Gamma_\infty$ for repulsion (K=2.52);

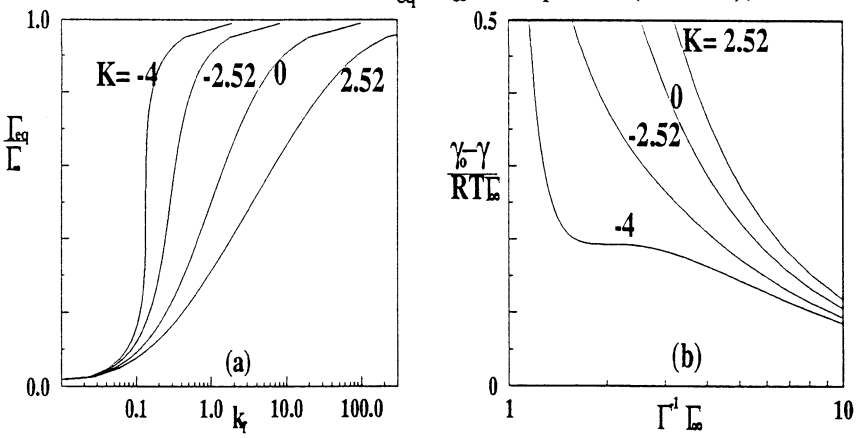

Figure 2 (a) Frumkin adsorption isotherm (b) surface equation of state

no interactions, (K=0, Langmuir); moderate cohesion (K=-2.52) and the elevated cohesion (K=-4.0), for which a plateau appears in the graph over a surface area range, indicating that the interface is approaching first-order surface phase change. The implications of this plateau in dynamic fluid particle systems is significant; an interface in this range of surface

concentrations may have gradients in Γ with negligible Marangoni effects.

3 Insoluble Surfactant Effects: Previous Results

The insoluble monolayer case has been studied at small Ca by Flummerfelt [7] and Stone and Leal [8]. The latter authors also studied surfactant effects at arbitrary Ca. The surfactant was assumed to obey a linear equation of state. All deformations are compared to a case where the surface tension remains constant at γ_{eq} throughout the deformation process. Fixing the product $E\Gamma_{eq}/\Gamma_\infty$, Marangoni effects are found to be pronounced at elevated Pe_s/Ca. Surfactant is swept to the drop tip and collects there, reducing the surface tension. The tip stretches, becoming elongated and curved to balance the normal stress jump. Greater deformations result for a given Ca, and reduced critical Ca^{cr} are realized. Conversely, at low Pe_s/Ca, near uniform Γ are maintained. Surface dilution causes γ to increase over γ_{eq}, strongly resisting surface dilatation. Smaller deformations at a given Ca, and higher Ca^{cr} are realized. At three fixed values of Pe_s/Ca, the parameter $E\Gamma_{eq}/\Gamma_\infty$ is increased. In general, as $E\Gamma_{eq}/\Gamma_\infty$ increases, larger Marangoni stresses retard v_s, and smaller Γ gradients result. Dilution of the interface dominates, so deformations are smaller at a given Ca, and Ca^{cr} is higher. For Pe_s/Ca up to 10, Ca^{cr} increases monotonically with $E\Gamma_{eq}/\Gamma_\infty$, and higher final deformations result. However, for Pe_s/Ca of 1000, non-monotonic behavior in $E\Gamma_{eq}/\Gamma_\infty$ in observed; Ca^{cr} is less than the uniform γ_{eq} case for small values of $E\Gamma_{eq}/\Gamma_\infty$, (where drop tip stretching dominates) and greater Ca^{cr} are found for larger values (where surface dilution dominates). This work was extended by Milliken, et al.[9] who used eqn (8) with K fixed at 2.52 in a finite drop deformation study. The deformations are compared to those found with the linear equation of state at the same initial surface coverage $\Gamma_{eq}/\Gamma_\infty$. Since eqn (8) gives lower γ for a given $\Gamma_{eq}/\Gamma_\infty$, larger deformations result.

4 Fluid Dynamics Equations and Solution Method

Using the radius a to scale lengths, Ga to scale velocity $\mathbf{v}_i$ in each phase, and γ_o/a to scale pressures, the flow is described by Stokes' equation:

$$Ca\nabla^2\boldsymbol{v}_i'=\nabla p_i'; \quad i=1,2 \tag{9}$$

$$\nabla\cdot\boldsymbol{v}_i'=0 \tag{10}$$

where 1,2, indicates droplet and external fluid quantities, respectively. The far-field boundary condition for $\mathbf{v}_1$' is the imposed extensional flow:

$$\lim_{x\to\infty} v_1' = v_\infty' = \begin{bmatrix} 2 & 0 & 0 \\ 0 & -1 & 0 \\ 0 & 0 & -1 \end{bmatrix} \cdot x' \qquad (11)$$

where x' is a position vector. The stream function for this flow is $\Psi' = -r'^2 z' Ca$, where r' and z' are the cylindrical radial and axial coordinates of a point in the fluid, respectively, as depicted in Fig. 1. The streamlines for this flow are symmetric hyperbolae. The boundary conditions at the interface are the stress balance, eqn (4), where $\gamma'(\Gamma'(x_s'))$ is determined by eqns (8) and (3), the continuity of velocity and the kinematic condition, given by:

$$\begin{aligned} v_1'(x_s') &= v_2'(x_s') = v_s'(x_s') \\ n \cdot v_s'(x_s') &= \frac{dx_s'}{dt'} \cdot n \end{aligned} \qquad (12)$$

where x_s' is the position vector of a point on the interface. Stokes' equations are recast as boundary integral equations over the surfaces enclosing the domains of flow. For an axisymmetric flow, the v_s' at x_s' is [cf3]

$$v_s'(x_s') = v_\infty'(x_s') - \frac{1}{8\pi}\int_s M'(x_s', \zeta') \cdot (\underline{T_1'} \cdot n - \underline{T_2'} \cdot n)\, ds'(\zeta') \qquad (13)$$

where **M'** is the axisymmetric Green's function for Stokes' flow, a second-order tensor, s' is the arclength and ζ' is a position vector on the interface, used as an integration variable.

The location of the drop interface is not known *a priori*. A time-marching numerical scheme is employed starting from an initially spherical drop. The initial conditions are that Γ' is unity, the tangential stress jump at the interface is zero, and the normal stress jump is given by $2\gamma_{eq}/\gamma_o$. The flow is initiated at a small capillary number Ca. Using the initial stress jump in eqn (13), $\mathbf{v}_s'$ is calculated at the first time step. The interface location is updated using eqn (12), and Γ' is updated using $\mathbf{v}_s$, and eqn (3) in an explicit Euler scheme. The stress jump is then updated using eqn (4), and the process is reiterated until $\mathbf{n} \cdot \mathbf{v}_s < .0005/Ca$, indicating that a steady shape has been attained. For all steady drop deformations, volume changes were less than 5%, and the total surfactant mass changed by less than .01%. The Ca is then incremented, and the process is repeated until $\mathbf{n} \cdot \mathbf{v}_s'$ fails to approach the convergence criterion or the drop volume increases by more than 10%, indicating drop fragmentation.

5 Results and Discussion

In Fig. 3(a), the surface concentration profile $\Gamma'(s')$ and surface tension gradients $\nabla_s \gamma'$ are presented for the steady shapes at Ca=0.024, where s' is normalized with the drop half-arc length. In order to compare with previous

results, we chose the conditions studied by Milliken et al. [9] ($\Gamma_{eq}/\Gamma_\infty$ = 0.2, Pe_s/Ca=1000 and E=1.5), who held K fixed at 2.52, i.e. repulsive interactions. This case, repeated by us, is shown, with the cases of no interaction (K=0), cohesion (K=-2.52), and strong cohesion (K=-4). In Fig. 3(b), deformation, defined in terms of drop length L and breadth B, is reported.

The insoluble monolayer limit corresponds to low C_{eq}. Referring to Fig. 2(a), these results correspond to different C_{eq} (or k_f, a dimensionless bulk concentration). For cohesion, (K=-4, k_f=.106; K-2.52, k_f =.155) low concentrations give $\Gamma_{eq}/\Gamma_\infty$ of 0.2, when compared to the cases of no interactions (K=0, k_f=.242) or repulsion, (K=2.52, k_f=.349).

The Γ' profiles in Fig. 3(a) are not symmetric about the K=0 case; cohesive interactions allow stronger Γ gradients to develop. Since γ is less sensitive to Γ for cohesion, smaller Marangoni stresses develop. Thus, surface convective flux remains strong, sweeping surfactant toward the tip.

The Marangoni stresses realized for K greater than -4 have the same general form; the stresses increase from the drop tip, reach a maximum and then decrease monotonically toward the equator. The strong cohesion case where K=-4 shows unusual behavior: the Marangoni stress *approaches zero when the surface concentration is within the plateau region in Fig. 2(b).*

Drop deformations as a function of Ca increase monotonically with K, because of reduced γ_{eq}. These data are presented in Fig. 3(b), inset, as a function of Ca_{eq} defined in terms of the γ_{eq} at each K. Referring to this inset, all deformations are higher than a reference case where γ is fixed throughout the deformation process at γ_{eq} corresponding to K=0. In Stone and Leal [8], deformation is discussed in terms of the competition of surface dilution resisting deformation and tip-stretching increasing it. These normal stress arguments explain much of the data. Since our results correspond to high Pe_s/Ca, γ is strongly reduced at the drop tip and tip-stretching dominates. In the inset to Fig. 3(b), the curves separate for Ca_{eq}>.025. The deformation decreases with increasing cohesion, a result of decreased surface tension gradients and diminished tip-stretching. For ease of comparison, $\Delta\gamma$', the difference between γ at the drop equator and drop tip normalized by γ_{eq}, is reported in Fig. 3(a) at Ca=.024. This difference monotonically decreases with increased cohesion at constant surface coverage.

For the case of moderate cohesion (K=-2.52) the deformation at higher surface coverage, $\Gamma_{eq}/\Gamma_\infty$=0.5, is reported in Fig. 3(b) as the dotted line (where E and Pe_s/Ca are held fixed). In terms of Ca, higher deformations develop because γ_{eq} is lower. However, when reported in terms of Ca_{eq}, (see inset) smaller deformations develop relative to the low coverage case. This occurs despite the strong $\Delta\gamma$' of 0.45, greater than that for $\Gamma_{eq}/\Gamma_\infty$=0.2. This result is *not* explained by tip-stretching or dilution. Rather, tangential Marangoni stresses compete with the normal stresses and reduce the deformation.

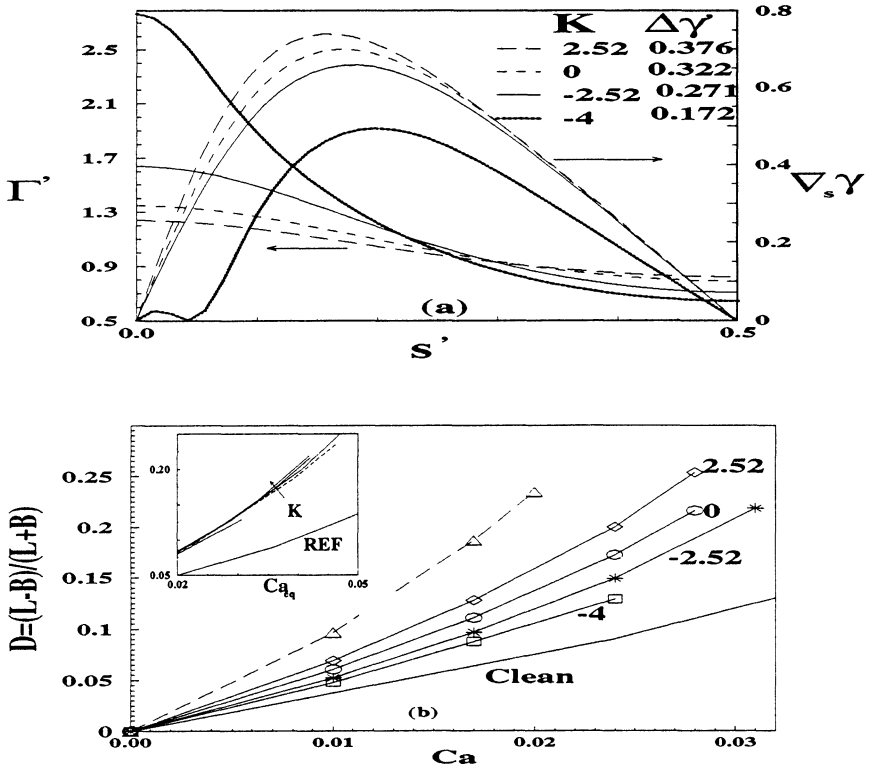

Figure 3: (a) Surface concentration and Marangoni stress profiles; (b) Steady deformations vs. Ca; inset: Steady deformations vs. Ca_{eq}

References

1. Taylor, G. I., Proc. R. Soc. London Ser., **A146**, 501 (1934)
2. Barthes-Biesel, D. and Acrivos, A., J. Fluid Mech, **61**, 1 (1973)
3. Rallison, J. M. and Acrivos, A., J. Fluid Mech., **89**, 191 (1978)
4. Levich, V.G. Physicochemical Hydrodynamics Prentice-Hall, Englewood Cliffs, N.J. (1962)
5. Lin, S.Y. et al. Langmuir **10**, 3442, (1994)
6. Aris, R. Vectors, Tensors, and the Basic Equations of Fluid Mechanics, Prentice-Hall, Englewood Cliffs, N.J. (1962)
7. Flummerfelt, R. W., J. Coll. Int. Sci., **76**, 330 (1980)
8. Stone, H. A. and Leal, L. G., J. Fluid Mech, **220**, 161 (1990)
9. Milliken, W., Stone, H. A. and Leal, L. G., Phys. Fluids A **5**, 69 (1993)